Proceedings of the ASME 2018 Dynamic Systems and Control Conference
DSCC2018
September 30-October 3, 2018, Atlanta, Georgia, USA

DSCC2018-9194

THE EFFECTS OF SWITCHING TIME ON SHARED HUMAN-ROBOT CONTROL

Roberto Belotti*
Facoltà di Scienze e Tecnologie
Libera Università di Bolzano
39100 Bolzano, Italia
Email: roberto.belotti@unibz.it

Karl von Ellenrieder
Facoltà di Scienze e Tecnologie
Libera Università di Bolzano
39100 Bolzano, Italia
Email: karl.vonellenrieder@unibz.it

ABSTRACT

In human-robot shared control, control authority is shared between human operators and automatic systems. Switching from one state to another can make the overall system unstable, even though the stability in each state is guaranteed. This issue is investigated in simulation using a Lane Keeping Assist System (LKAS), which guides a vehicle along a lane, while allowing lane changes, if desired by the human. An interface allows a human to input a steering control signal with a joystick and provides visual feedback of lane-position. The total steering command is the combination of the LKAS control signal and the human steering input. System performance is explored as the vehicle switches among different levels of cooperation between the human and the automatic driving system. The minimum time permitted between lane changes is an important parameter. As this time is decreased, user intent and the automatic controller are in conflict more often, resulting in larger control efforts from both user and automatic controller.

NOMENCLATURE

a Distance of the center of gravity from the rear axle
b Wheel base
β Sideslip angle
δ Front wheel steering angle
v Speed of the center of gravity
ψ Heading of the vehicle
(X,Y) Position of the center of gravity in the inertial reference frame

INTRODUCTION

In several branches of robot control, including but not limited to mobile robot guidance, human-machine cooperation has become a fertile field of investigation. On one hand, purely autonomous systems perform particularly well in static and structured environments. On the other hand, human control is often more suited to dynamically changing and uncertain conditions, since humans are more flexible and adaptable.

There are several situations in which the overall goal of the system can be broken down into different subtasks. In order to take advantage of the capabilities of each member of the human-machine team, it is convenient to define a framework for the shared authority over the execution of tasks. Such a framework may include the use of *sliding autonomy*, in which various subtasks may be performed autonomously by the machine, under the human control, or semi-autonomously, using so-called *shared control*, in which the system receives a combined control input from both the human user and the automatic control system.

Usually, only discrete levels of shared control are considered [1], but could also include continuously adjustable levels [2]. Examples of existing systems with continuously adjustable autonomy include lane-keeping assistive systems and adaptive cruise control systems for automobiles [3, 4]. Other examples are space operations [5, 6], industrial robotics [7] and map-building [8, 9]. In such systems, the initiative [10] for performing the task may switch between human and machine.

Continuous-time systems with discrete switching events are known in the literature as *switched systems*. It has been observed that a switched system can be destabilized, even though all individual subsystems are stable [11]. A classical approach

*Address all correspondence to this author.

in time-dependent switching relies on the fact that stability can be guaranteed among stable subsystems, provided that each subsystem remains active for a certain dwell-time τ_d. Heuristically, the dwell-time should be at least as long as the settling time of the slowest part of the system. This concept was later refined in [12], where it is proven that stability is assured as long as each subsystem remains active for an average of τ_d.

Recently, many switched system based approaches have appeared in the literature, and several problems in different fields (including but not limited to vehicle control) have been tackled exploiting switched systems. An example of unmanned surface vehicle control, which includes validation in field experiments, is presented in [13]. In [14], a gear shifting strategy to improve the fuel efficiency of hybrid electric vehicles is transformed into an optimal control problem for a switched system. The stabilization of non-linear systems in the presence of disturbances using switching controllers has been addressed in [15], where the proposed methodology is also applied to the dynamic model of an underactuated autonomous underwater vehicle. In [16], a switched polytopic system with locally overlapped switching law is established to describe flight dynamics. In [17] an antilock braking system controller is presented, which employs a switched control strategy, to take the discontinuous dynamics of hydraulic actuators into account.

In order to explore the effects of dwell time on a switched shared human-robot system, a lane-keeping assist system (LKAS) is studied here. The method has been recently introduced in the automotive industry and concerns the retention of the expected trajectory by properly steering when a car detects itself drifting out of its lane. In this work, a user-intent detection technique that relies on steering wheel angle measurements is presented. The approach is inspired by [4], in which torque measurements are employed, instead. Numerical simulations are performed to explore how varying dwell time can affect system performance.

APPROACH

The proposed shared-control scheme is represented by the diagram in Fig. 1, in which the main functional blocks of the developed LKAS are shown, together with the exchanged information among them. The aim of this section is to give the details on the implementation of each block.

Steering model

A simple kinematic model is employed to represent vehicle steering, under the assumption that no slipping of the wheels occurs. Such a model is the classic bicycle model [18], obtained by lumping the front (rear) pair of wheels into a single front (rear) wheel. The resulting system is represented in Fig. 2. The relation between sideslip angle β and steering angle δ is

$$\beta = \arctan\left[\frac{a\tan(\delta)}{b}\right], \tag{1}$$

where b is the distance between the front and rear axles, a is the distance between the rear axle and the center of gravity of the car. The equations of motion of the center of gravity of the vehicle are

$$\dot{X} = v\cos(\beta+\psi), \tag{2}$$

$$\dot{Y} = v\sin(\beta+\psi), \tag{3}$$

where v is the speed of the car and ψ is its heading. From Fig. 2, the relation between steering angle and yaw rate can be seen to be

$$\dot{\psi} = \frac{v}{b}\tan\delta. \tag{4}$$

By linearizing (3) about $(Y=0, \psi=0)$, using (1) and assuming small steering angles in (4), a quasi one dimensional model the of the vehicle's trajectory can be developed, which gives the system

$$\begin{aligned}\dot{Y} &= v_0\psi + \frac{av_0}{b}\delta,\\ \dot{\psi} &= \frac{v_0}{b}\delta,\end{aligned} \tag{5}$$

where the speed of the car is taken to be the constant v_0. This model assumes Y represents small lateral deviations from the vehicle's path along the X axis.

The two equations in the system in (5) can be combined to model the car as a linear single input, single output (SISO) system with the transfer function $G(s)$ between output Y and input steering angle δ. The transfer function is given by

$$G(s) = \frac{\mathscr{Y}}{\Delta} = \frac{av_0}{b}\frac{(s+v_0/a)}{s^2}, \tag{6}$$

where s is the Laplace transform variable, $\mathscr{Y} = \mathscr{L}\{Y\}$ is the Laplace transform of the lateral distance, and $\Delta = \mathscr{L}\{\delta\}$ is the Laplace transform of the steering angle.

Supervisor

The supervisor is devoted to two important tasks. First of all, it determines whether the human driver and the Driving Assistance System (DAS), i.e. the autonomous steering system for

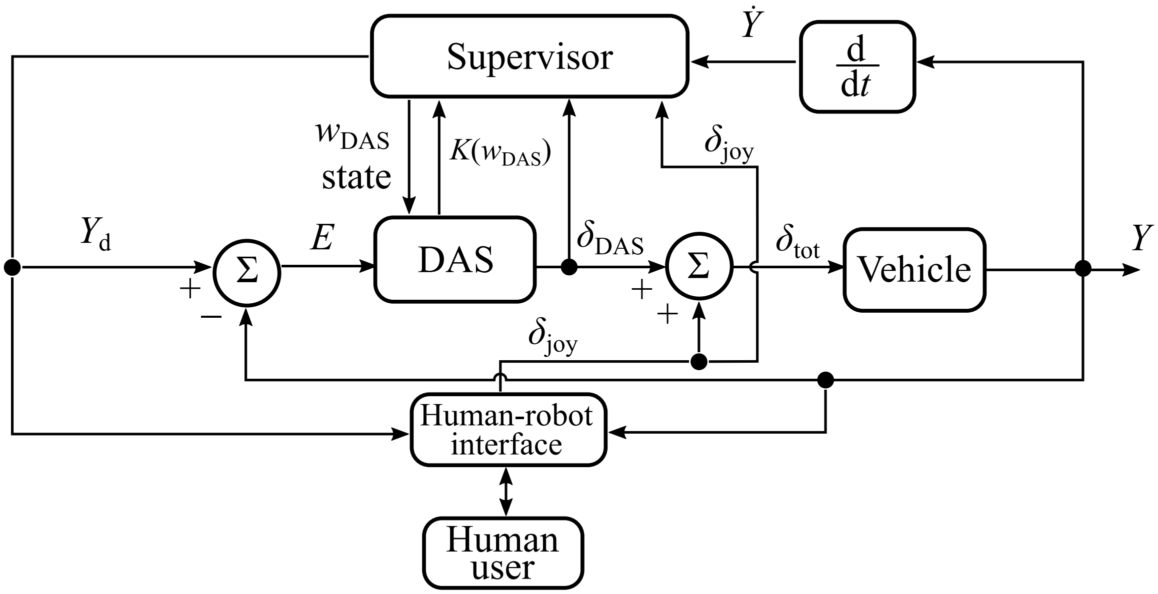

FIGURE 1. BLOCK DIAGRAM OF THE LKAS.

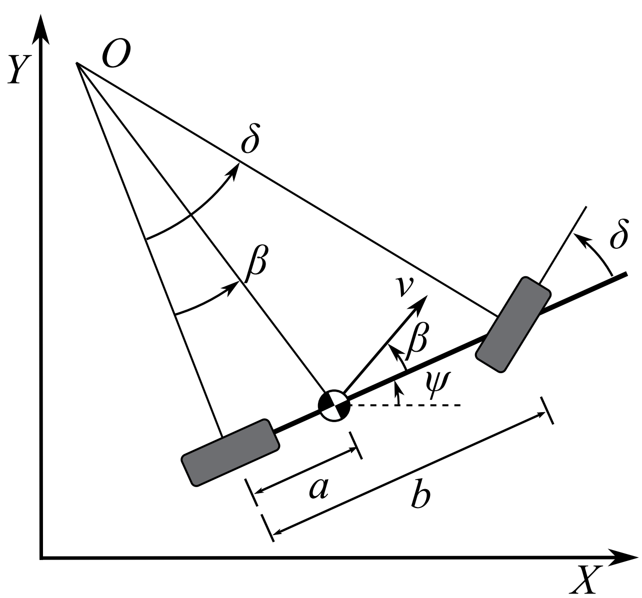

FIGURE 2. THE BICYCLE MODEL. POINT O IS THE INSTANTANEOUS RADIUS OF TURNING. AS IS COMMON, THE RADII FROM O TO THE FRONT WHEEL, REAR WHEEL AND CENTER OF GRAVITY ARE APPROXIMATED AS EQUAL. THE HEADING ANGLE ψ IS MEASURED BETWEEN THE CENTERLINE OF THE VEHICLE AND THE X (EAST) AXIS.

lane keeping, are cooperating or not, based on their respective driving choices. Moreover, the supervisor detects the intent of the user to change lanes and adjust the reference trajectory for the DAS accordingly. The methodology that is used to evaluate the human-DAS cooperation relies on the haptic-based approach presented in [4]. The figures of merit considered are

$$w_{\text{joy}}(t) = \frac{1}{\Delta T}\int_{t-\Delta T}^{t} \delta_{\text{joy}}(\eta)\,\dot{Y}(\eta)\,\mathrm{d}\eta, \tag{7}$$

and

$$w_{\text{DAS}}(t) = \frac{1}{\Delta T}\int_{t-\Delta T}^{t} \delta_{\text{DAS}}(\eta)\,\dot{Y}(\eta)\,\mathrm{d}\eta, \tag{8}$$

where δ_{joy} and δ_{DAS} are the front wheel steering angle control signal from the joystick and the DAS controller, respectively. Given the adopted convention for axes orientation, the integrand functions in (7) and (8) are positive if the vehicle is turning consistently with the steering wheel angle required by either the human operator or the DAS, and they are negative otherwise. Therefore, it is reasonable to define the following states:

- I Human-led cooperative state, which occurs when $w_{\text{joy}} \geq 0$ and $w_{\text{DAS}} \geq 0$, i.e. the human operator is holding the initiative and the DAS agrees with him/her.
- II Human-led uncooperative state, which occurs when $w_{\text{joy}} \geq 0$ and $w_{\text{DAS}} < 0$, i.e. the human operator is holding the initiative and the DAS does not agree with him/her.
- III System-led state, which occurs when $w_{\text{joy}} < 0$, i.e. the DAS is holding the initiative.

Driving Assistance System

In order to help the human track the center of a desired lane, the DAS provides a control input δ_{DAS}, which is combined with the human input δ_{joy}. The DAS control signal is given by

$$\delta_{\text{DAS}} = K(w_{\text{DAS}})e, \tag{9}$$

where $e := Y - Y_d$ is the trajectory error and $K(w_{\text{DAS}})$ is a variable-gain given by

$$K(w_{\text{DAS}}) = \begin{cases} \dfrac{K_0}{1+\exp(-\rho w_{\text{DAS}} + \sigma)}, & \text{state II} \\ K_0, & \text{otherwise.} \end{cases} \tag{10}$$

In practice, the gain is constant unless the human operator is forcing the vehicle against the DAS (State II). In that case, the gain is decreased by a factor, which depends on w_{DAS} and that becomes zero for $-w_{\text{DAS}} \gg 0$. The parameters ρ and σ are tuned to make the transition from K_0 to 0 as smooth as possible.

The value of K_0 is chosen by examining the closed loop roots of the characteristic equation $1 + K_0 G(s) = 0$, where $G(s)$ is given by (6). The system is a classical second order system, which can be expressed in the canonical form $s^2 + 2\zeta\omega_n s + \omega_n^2 = 0$, where ζ is the damping ratio and ω_n is the natural frequency of the system. To obtain a fast response with relatively little overshoot, the closed loop roots are selected so that $\zeta = 1/\sqrt{2}$ by taking

$$K_0 = \frac{4b\zeta^2}{a^2} = \frac{2b}{a^2}. \tag{11}$$

The resulting theoretical value of the 2% settling time is $t_s = 4a/v_0$. In order to ensure that unrealistically large steering angles are not commanded, the output of the DAS controller is saturated to the range $-45^\circ \leq \delta_{\text{DAS}} \leq 45^\circ$. Of course, when the steering angle is at one of its saturation limits, the effective controller gain is reduced, which causes an associated decrease of the effective damping ratio. This, in turn, results in a larger overshoot and longer settling time than that predicted by linear theory.

As shown in Fig. 1, the steering angle output by the DAS and commanded by the user are combined. Owing to the configuration of the joystick, the steering angle commanded by the human user is limited to $-45^\circ \leq \delta_{\text{joy}} \leq 45^\circ$. A second saturation block is used on the combined signal δ_{tot}, to ensure that the sum of the steering angles is limited to $-45^\circ \leq \delta_{\text{tot}} \leq 45^\circ$ (Fig. 3).

Lane change

The supervisor is also responsible for detecting the human operator's intent to change lanes. The condition for assessing intent is

$$K(w_{\text{DAS}}) \leq \alpha^2 K_0, \tag{12}$$

where α is a constant that can be chosen according to specific design needs. When (12) is fulfilled, the target trajectory Y_d is shifted by the distance ΔY to match the center of the next lane, either to the right or to the left of the vehicle's position. Hence,

$$Y_d = \begin{cases} Y_{\text{current}} - \Delta Y, & \text{if } \dot{Y} < 0 \\ Y_{\text{current}} + \Delta Y, & \text{if } \dot{Y} > 0 \\ Y_{\text{current}}, & \text{otherwise.} \end{cases} \tag{13}$$

A lane change is not permitted at time t if the preceding lane change occurred after the time $t - T_{\min}$. Since lane changes can only occur in state II (uncooperative), this waiting time allows the system to complete a lane change and return to cooperative status before the next lane change is initiated.

Human-robot interface

The aim of the human-robot interface is to provide the human user with an adequate awareness of the vehicle situation and also the DAS intent, by showing visual feedback of the vehicle current position and the reference trajectory on a screen. Moreover, the interface includes a joystick, so the human operator could steer right or left as desired. The employed human-robot interface can be considered as a teleoperated system [19]. Teleoperation is connected to some issues that have been often addressed in the recent literature. One such issue is maintaining stability regardless of how the operator and/or the environment act on the system. Typically, arguments for proving stability rely on the concept of passivity [20]. The dynamical system (5) is said to be *passive* if there exists a continuously differentiable semidefinite scalar function $V(t) = V(Y(t), \Psi(t))$ (called the storage function) such that $\dot{V} \leq \delta Y$, namely

$$V(t) - V(0) \leq \int_0^t \delta(\eta) Y(\eta)\, \mathrm{d}\eta, \qquad \forall t \geq 0. \tag{14}$$

Passivity of the teleoperated system is desirable because if the human operator and the environment are also passive, passivity of the closed-loop system is guaranteed and therefore also stability is assured.

METHOD VALIDATION

The proposed method has been validated with numerical experiments. The LKAS has been implemented with the commercial software Simulink by Mathworks. The resulting model is

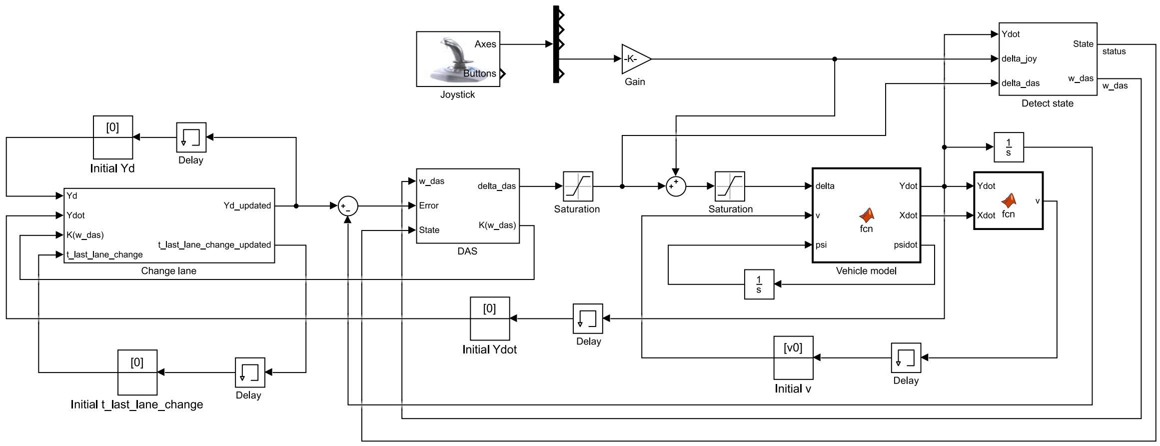

FIGURE 3. SIMULINK MODEL OF THE LKAS.

TABLE 1. PARAMETER VALUES USED IN THE TESTS.

Parameter	Value
a [m]	0.5
b [m]	1
v_0 [m/s]	1
ΔT [s]	1
α^2	0.3
ΔY [m]	1
ρ	10
σ	0.4

shown in Fig. 3. It has been considered a vehicle traveling East for $T_f = 40$s on a road having a virtually unlimited number of lanes. The parameters previously described have been chosen as in Tab. 1. Such values are chosen given the prospect of doing an experimental validation using 1:5 scale RC ground vehicles in the near future. The inequalities (7) and (8) that define states I, II and III, which are theoretically valid, have been conservatively enforced, in order to prevent misjudgment due to noise in the joystick signal acquisition. In practice, the following definitions are used:

$$\begin{aligned} \text{State I: } & w_{\text{joy}} \geq -0.2, \quad w_{\text{DAS}} \geq -0.1 \\ \text{State II: } & w_{\text{joy}} \geq -0.2, \quad w_{\text{DAS}} < -0.1 \\ \text{State III: } & w_{\text{joy}} < -0.2. \end{aligned} \tag{15}$$

The aim of the tests that are shown in the present Section is to evaluate how the choice of $T_{\min}$ affects the stability of the system. To this end, the joystick input signal has been recorded during one test, setting $T_{\min} = 5$s, and then the simulation have been repeated for different values of $T_{\min}$.

The quantities that have been evaluated are: the lateral position $Y(t)$ of the vehicle (i.e. in the North-South direction), compared with the desired trajectory $Y_d(t)$, as computed by the Driving Assistance System; the state detected by the supervisor; the proportional gain $K(w_{\text{DAS}})$; the steering angles δ_{joy} and δ_{DAS}; and finally w_{joy} and w_{DAS}.

Such quantities are shown in Fig. 4 and 5 for $T_{\min} = 5$s and $T_{\min} = 3$s respectively. In the first case, the actual trajectory of the car tracks closely the desired one. There are some small gaps between the two trajectories, which are due to either driver's own choice or overshooting (the actual cause can be identified by inspection of the plot of δ_{joy}). In the second case, instead, there are major discrepancies between the desired trajectory and the obtained one, so the DAS fails to track the desired trajectory. Moreover, the numerous lane changes that happen over a short timespan in the second test suggest that the system may not be asymptotically stable for some human control-inputs.

Moreover, it is important to notice that State III does not occur in the first test, but it does in the second one. In such a circumstance, the vehicle is led by the DAS, regardless of whether the human operator is cooperating or not. Also State II, i.e. human-led uncooperative state, occurs for very short time periods if $T_{\min} = 5$s, with the system promptly returning to cooperative state as soon as the DAS detects the intent to change lane, while for $T_{\min} = 3$s State II remains active for a significantly longer timespan. This is an additional evidence of relevance of the choice of $T_{\min}$ to the performance of the LKAS.

Further insights on the driver intent detection are provided by the third plot, in which $K(w_{\text{DAS}})$ is shown: it is possible to notice that in State II the gain is gradually decreased and the gain falling below the threshold of Eq. (12) (represented by a dashed line) triggers a lane change, whenever it is allowed. Finally, the cooperative behavior can be assessed in the fifth plot: in fact in the second example w_{joy} and w_{DAS} are greater in magnitude with respect to the first example, suggesting that the human operator and the DAS are putting more effort in opposing each other. In the latter plot, dashed lines represent the enforced thresholds of Eq. (15).

CONCLUDING REMARKS

A simulation of a lane keeping driver assist system has been developed using a kinematic bicycle model, which permits a user to follow a trajectory using a joystick. When the shared control system detects that the user's intent is to change lanes, the system automatically reduces its control effort in the prior lane and increases the effort it generates to help guide the user towards the new selected lane. The elapsed time between lane changes is constrained to be more than $T_{\min}$. It is found that when $T_{\min}$ is low, the system spends more time in a computer-led non-cooperative state wherein user intent and automatic control are in conflict. This results in larger control efforts on both the part of the user and the automatic controller. Although not the same quantity, the time $T_{\min}$ seems to be related to the minimum dwell time τ_d for state switching in hybrid systems. Further work is required to clarify the relationship between these quantities.

REFERENCES

[1] Sheridan, T. B., and Verplank, W. L., 1978. Human and computer control of undersea teleoperators. Tech. rep., DTIC Document.

[2] Abbink, D. A., Mulder, M., and Boer, E. R., 2012. "Haptic shared control: smoothly shifting control authority?". *Cognition, Technology & Work,* ***14***(1), pp. 19–28.

[3] Tsoi, K. K., Mulder, M., and Abbink, D. A., 2010. "Balancing safety and support: Changing lanes with a haptic lane-keeping support system". In Systems Man and Cybernetics (SMC), 2010 IEEE International Conference on, IEEE, pp. 1236–1243.

[4] Nishimura, R., Wada, T., and Sugiyama, S., 2015. "Haptic shared control in steering operation based on cooperative status between a driver and a driver assistance system". *Journal of Human-Robot Interaction,* ***4***(3), pp. 19–37.

[5] Dorais, G., Bonasso, R., Kortenkamp, D., Pell, B., and Schreckenghost, D., 1998. "Adjustable autonomy for human-centered autonomous systems on Mars". *Proceedings of the First International Conference of the Mars Society*, pp. 397–420.

[6] Sierhuis, M., Bradshaw, J. M., Acquisti, R., Van Hoof, R., and Jeffers, R., 2003. "Human-agent teamwork and adjustable autonomy in practice". In Proceedings of the Seventh International Symposium on Artificial Intelligence, Robotics and Automation in Space.

[7] Kortenkamp, D., Burridge, R., Bonasso, P., Schrenkenghost, D., and Hudson, M., 1999. "An intelligent software architecture for semiautonomous robot control". *Proc. Autonomy Control Software Workshop, Autonomous Agents*.

[8] Nielsen, C., Goodrich, M., and Crandall, J., 2003. "Experiments in human-robot teams". *Multi-Robot Systems: From Swarms to Intelligent Automata,* ***2***.

[9] Crandall, J. W., Goodrich, M. A., Olsen, D. R., and Nielsen, C. W., 2005. "Validating human-robot interaction schemes in multitasking environments". *IEEE Transactions on Systems, Man, and Cybernetics-Part A: Systems and Humans,* ***35***(4), pp. 438–449.

[10] Sellner, B., Heger, F. W., Hiatt, L. M., Simmons, R., and Singh, S., 2006. "Coordinated multiagent teams and sliding autonomy for large-scale assembly". *Proceedings of the IEEE,* ***94***(7), pp. 1425–1444.

[11] Liberzon, D., 2012. *Switching in systems and control*. Springer Science & Business Media.

[12] Hespanha, J. P., and Morse, A. S., 1999. "Stability of switched systems with average dwell-time". In Decision and Control, 1999. Proceedings of the 38th IEEE Conference on, Vol. 3, IEEE, pp. 2655–2660.

[13] Bertaska, I. R., and von Ellenrieder, K. D., 2018. "Experimental evaluation of supervisory switching control for unmanned surface vehicles". *IEEE Journal of Oceanic Engineering*.

[14] Fang, L., and Qin, S., 2006. "Optimal control of parallel hybrid electric vehicles based on theory of switched system". *Asian Journal of Control,* ***8***(3), pp. 274–280.

[15] Aguiar, A. P., Hespanha, J. P., and Pascoal, A. M., 2007. "Switched seesaw control for the stabilization of underactuated vehicles". *Automatica,* ***43***(12), pp. 1997–2008.

[16] Hou, Y., Wang, Q., and Dong, C., 2011. "Gain scheduled control: switched polytopic system approach". *Journal of Guidance, Control, and Dynamics,* ***34***(2), pp. 623–629.

[17] Jing, H., Liu, Z., and Chen, H., 2011. "A switched control strategy for antilock braking system with on/off valves". *IEEE Transactions on Vehicular Technology,* ***60***(4), pp. 1470–1484.

[18] Aström, K. J., and Murray, R. M., 2010. *Feedback systems: an introduction for scientists and engineers*. Princeton university press.

[19] Hokayem, P. F., and Spong, M. W., 2006. "Bilateral teleoperation: An historical survey". *Automatica,* ***42***(12), pp. 2035–2057.

[20] Desoer, C. A., and Vidyasagar, M., 1975. *Feedback systems: input-output properties*, Vol. 55. Siam.

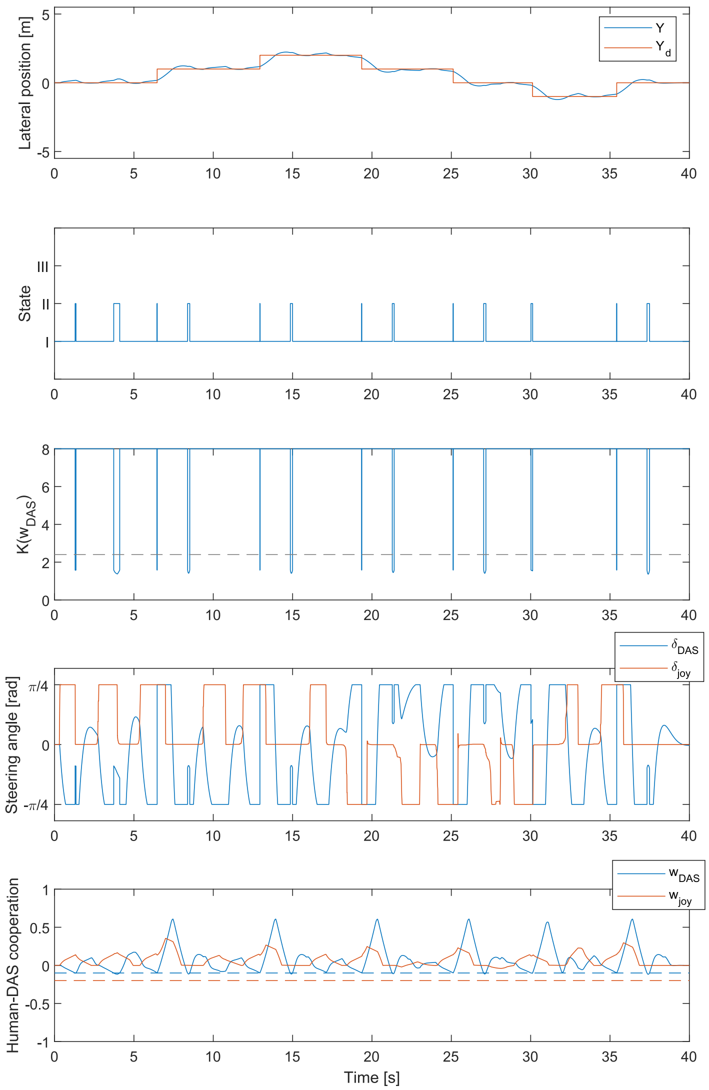

FIGURE 4. PERFORMANCE EVALUATION OF LKAS FOR $T_{\mathrm{MIN}} = 5$S. NOTE, LANE CHANGES ARE NOT PERMITTED DURING THE INITIAL 5 SECONDS OF THE SIMULATION. DASHED LINE IN THE THIRD PLOT REPRESENTS RIGHT-HAND SIDE OF INEQUALITY (12). DASHED LINES IN THE FIFTH PLOT REPRESENT ENFORCED THRESHOLD IN (15).

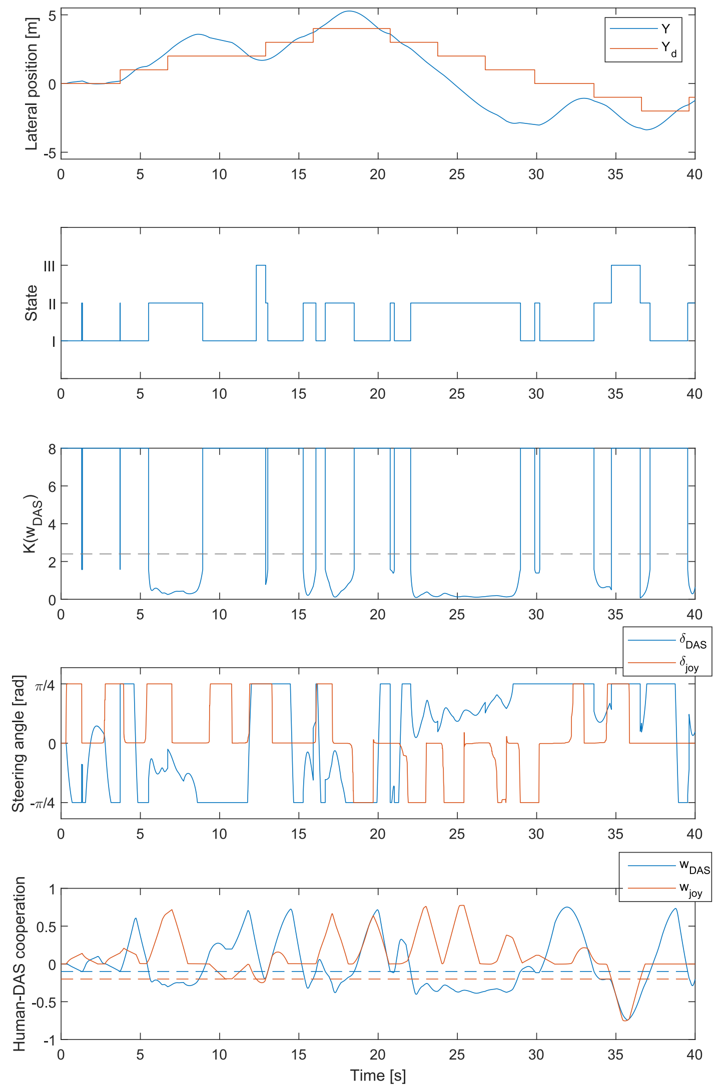

FIGURE 5. PERFORMANCE EVALUATION OF LKAS FOR $T_{\mathrm{MIN}} = 3$S. NOTE, LANE CHANGES ARE NOT PERMITTED DURING THE INITIAL 3 SECONDS OF THE SIMULATION. DASHED LINE IN THE THIRD PLOT REPRESENTS RIGHT-HAND SIDE OF INEQUALITY (12). DASHED LINES IN THE FIFTH PLOT REPRESENT ENFORCED THRESHOLD IN (15).